Abbassi, A., Cipollari, P., Fellin, M.G., Zaghloul, M.N., Guillong, M., El Mourabet, M., and Cosentino, D., 2021, The Numidian sand event in the Burdigalian foreland basin system of the Rif, Morocco, in a source-to-sink perspective: GSA Bulletin, https://doi.org/10.1130/B36136.1.

Supplemental Material

Figure S1. Accumulate thickness-age diagram with the comparison of the final thickness with the results of the original accumulate thickness of the pre- and syn-orogenic deposits after decompaction, by using the porosity change method (Bond et al., 1983). For detailed lithologies and successions: the Tanger Unit is after Zaghloul et al. (2005), Chalouan et al. (2008), Abbassi et al. (2020), Personal commun., 2020; the Ketama Unit is after Durand-Delga and Olivier (1988); the Beni Ider Unit is after Durand-Delga and Olivier (1988), Zaghloul et al. (2007), and this work; the Tisiren Unit is after Durand-Delga et al. (1999); and the Predorsalian Unit is after Durand-Delga and Olivier (1988), Durand-Delga and Maaté (2003), and this work.

Figure S2. Sub-Numidian (Varicolored Clays) stratigraphic log (35°31'57.88"N, 5°50'11.85"W) showing the calcareous nannofossils marker species found in the Varicolored Clays below the - "Numidian Facies" of the 9th April 1947 Dam section. Red dots in the sample column show barren samples.

Figure S3. Stratigraphic log of the Supra-Numidian deposits (35°32'46,26"N, 5°50'01.74"W) above the "Numidian Facies" of the 9th April 1947 Dam section and quantitative analyses (abundance percentages) of calcareous nannofossils selected taxa. The first occurrence (FO) of *S. belemnos* is also shown.

Figure S4. Calcareous nannofossils plate showing the marker species recognized in the study sections: **(A)** *Discoaster druggii*, sample Sub 17 (Varicolored Clays; 9th April 1947 Dam section, "Numidian Facies"); **(B)** *Helicosphaera carteri*, sample SN 23 (Supra-Numidian deposits; 9th April 1947 Dam section, "Numidian Facies"); **(C)** *Helicosphaera carteri*; sample AB 23 (Imâm Rhìt section; "Mérinides Facies")**; (D)** *Helicosphaera carteri*; sample PD 1 (Al Fahamine section; "Beliounis Facies"); **(E)** *Helicosphaera ampliaperta*; samples AB 21 (Imâm Rhìt section; "Mérinides Facies"); **(F-G)** *Helicosphaera ampliaperta*, sample SN 9 (Supra-Numidian deposits; 9th April 1947 Dam section, "Numidian Facies"), **(F)** crossed nicols 0°, **(G)** crossed nicols 45°; **(H)** *Helicosphaera ampliaperta*; sample AB 33 (Imâm Rhìt section; "Mérinides Facies"); **(I)** *Helicosphaera mediterranea*; sample AB 16 (Imâm Rhìt section; "Mérinides Facies"); **(J)** *Helicosphaera mediterranea*, sample SN 3 (Supra-Numidian deposits; 9th April 1947 Dam section, "Numidian Facies"); **(K)** *Helicosphaera mediterranea*, sample PD 1 (Al Fahamine section; "Beliounis Facies"); **(L-M)** *Sphenolithus delphix*, sample Sub 13 (Varicolored Clays; 9th April 1947 Dam section, "Numidian Facies"); **(L)** crossed nicols 0°; **(M)** crossed nicols 45°; **(N-O)** *Sphenolithus disbelemnos*, sample AB 21 (Imâm Rhìt section; "Mérinides Facies"); **(N)** crossed nicols 0°; **(O)** crossed nicols 45°; **(P-Q)** *Sphenolithus disbelemnos*, sample SN 1 (Supra-Numidian deposits; 9th April 1947 Dam section, "Numidian Facies"); **(P)** crossed nicols 0°; **(Q)** crossed nicols 45°; **(R-T)** *Sphenolithus belemnos*, sample SN 15 (Supra-Numidian deposits; 9th April 1947 Dam section, "Numidian Facies"); **(R)** crossed nicols 0°; **(S)** crossed nicols 15°; **(T)** crossed nicols 45°.

Figure S5. Stratigraphic log of the Imâm Rhìt section ("Mérinides Facies") (35°30'30.20"N, 5°39'20.42"W), and quantitative analyses (abundance percentages) of calcareous nannofossils selected taxa. Red dots in the sample column show barren samples.

Figure S6. Stratigraphic log of the Al Fahamine section ("Beliounis Facies") (35°44'38.08" N, 5°32'11.81"W), and marker species recognized in the section. Red dots in the sample column show barren samples.

Figure S7. Stratigraphic panel showing the main pre-orogenic stratigraphic successions of the substratum of the Burdigalian foreland basin system of the Rif Chain.

Table S1. Nannofossils countings from the Supra-Numidian deposits of the 9th April 1947 Dam section, representative of the "Numidian Facies".

Table S2. Nannofossils countings from the Imâm Rhìt section, representative of the "Mérinides Facies".

Table S3. Point-count raw (Excel File-Sheet 1) and recalculated modal point-count data (Excel File-Sheet 2) of three stratigraphic sections: 9th April 1947 Dam section ("Numidian Facies"), Imâm Rhìt section ("Mérinides Facies"), and Boulaichiches sections ("Beliounis Facies").

Table S4. Results of U-Th-Pb LA-ICP-MS analyses and calculated ages for zircon separates from the sandstones samples of 9th April 1947 Dam section ("Numidian Facies"; Excel File-Sheet ZBS1/ZBS2), Imâm Rhìt section ("Mérinides Facies"; Excel File-Sheet ZBH1/BNI1/ZBH2), and Boulaichiches sections ("Beliounis Facies"; Excel File-Sheet ZPD).

Table S5. Trace and REE elements of zircon separates from the sandstones samples of 9th April 1947 Dam section ("Numidian Facies"; Excel File-Sheet ZBS1/ZBS2), Imâm Rhìt section ("Mérinides Facies"; Excel File-Sheet ZBH1/BNI1/ZBH2), and Boulaichiches sections ("Beliounis Facies"; Excel File-Sheet ZPD).

Table S6. Results of the decompaction technique of the pre- and syn-orogenic deposits of the Burdigalian foreland basin system of the Rif Chain, obtained by using the porosity-depth change method illustrated in Bond et al. (1983). For detailed lithologies and successions: the Tanger Unit is after Zaghloul et al. (2005), Chalouan et al. (2008), Abbassi et al. (2020), Personal commun., 2020; the Ketama Unit is after Durand-Delga and Olivier (1988); the Beni Ider Unit is after Durand-Delga and Olivier (1988), Zaghloul et al. (2007), and this work; the Tisiren Unit is after Durand-Delga et al. (1999); and the Predorsalian Unit is after Durand-Delga and Olivier (1988), Durand-Delga and Maaté (2003), and this work.

INTRODUCTION

The additional **Figure S1 and Table S6** show the subsidence curves and sedimentation rates of Ketama-Tanger, Tisiren-Beni Ider, and Predorsalian units. The compaction history to detect the original and final porosity was performed by using the diagrams from Bond et al. (1983). **Figures S2 to S6 and tables S1 to S2** show the biostratigraphy and the quantitative analyses carried out on calcareous nannofossils from three stratigraphic sections: 9th April 1947 Dam section ("Numidian Facies"), Imâm Rhìt section ("Mérinides Facies"), and Al Fahamine

and Boulaichiches sections ("Beliounis Facies"). The micropaleontologic analyses were performed at the Laboratory of Stratigraphy of Roma Tre University, from September 2019 to October 2020. Details on the methods followed to perform the analyses are reported in section "**Biostratigraphic analysis**" of the main text of the paper. The micropaleontologic analyses of the 9th April 1947 Dam section ("Numidian Facies", representative for the foreland), of the Imâm Rhìt section ("Mérinides Facies", representative for the foredeep), and of the Al Fahamine section ("Beliounis Facies", representative for the wedge-top) allow us to constrain the arrival of the quartz grains of both the Numidian and Numidian-like deposits to an age younger than the FO of *H. mediterranea* (ca. 20 Ma, early Burdigalian). In addition, the presence in the Supra-Numidian deposits of *H. mediterranea*, *H. ampliaperta*, together with the FO of *S. belemnos,* indicates that the arrival of quartz grains ended before 19 Ma, demonstrating that the Numidian sand event in Northern Morocco occurred in less than 1 Myr. **Figure S7** is a stratigraphic panel showing the main pre-orogenic stratigraphic successions of the substratum of the Burdigalian foreland basin system of the Rif Chain. **Table S3** shows the point-count raw and the recalculated modal point-count data for three stratigraphic sections: 9th April 1947 Dam section ("Numidian Facies"), Imâm Rhìt section ("Mérinides Facies"), and Boulaichiches sections ("Beliounis Facies"). The quantitative petrographic analyses were performed at the ESRG laboratory of Department des Sciences de la Terre, University Abdelmalek Essaadi, Tanger, Morocco. Details on the methods followed to perform the analyses are reported in section "**Petrographic analyses**" of the main text of the paper. **Table S4** shows the results of U-Th-Pb LA-ICP-MS analyses and calculated ages for zircon separates from the sandstones samples of 9th April 1947 Dam section ("Numidian Facies"), Imâm Rhìt section ("Mérinides Facies"), and Boulaichiches sections ("Beliounis Facies"). Data in yellow marker (Excel file) were discarded based on the $^{206}Pb/^{238}U$ uncertainty above 5%. The analysis label in the first column is composed by adding in sequence the number of the sample, of the mount, of the grain and finally of the U-Pb analysis on the same grain so that multiple U-Pb analysis on the same grain are indicated by the last sequence number of the label. The Detrital Zircon U-Pb geochronologic analyses were performed at Institute of Isotope Geochemistry and Petrology (IGP), ETH Zurich. Details on the methods followed to perform the analyses are reported in section "**Detrital zircon U-Pb geochronology analyses**" of the main text of the paper. **Table S5** shows the trace and REE elements of zircon of sandstone samples collected from 9th April 1947 Dam section ("Numidian Facies"), Imâm Rhìt section ("Mérinides Facies"), and Boulaichiches sections ("Beliounis Facies") as obtained through in situ LA-ICPMS analyses. The trace and REE elements were performed at Institute of Isotope Geochemistry and Petrology (IGP), ETH Zurich. Details on the methods followed to perform the analyses are reported in section "**Detrital zircon U-Pb geochronology analyses**" of the main text of the paper.

REFERENCES CITED

Abbassi, A., Cipollari, P., Zaghloul, M.N., and Cosentino, D., 2020, The Rif Chain (Northern Morocco) in the Late Tortonian-Early Messinian Tectonics of the Western Mediterranean Orogenic Belt: Evidence from the Tanger-Al Manzla Wedge-Top Basin: Tectonics, v. 39, https://doi.org/10.1029/2020TC006164.

Bond, G.C., Kominz, M.A., and Devlin, W.J., 1983, Thermal subsidence and eustasy in the lower Paleozoic miogeocline of western North America: Nature, v. 306, p. 775–779, https://doi.org/10.1038/306775a0.

Chalouan, A., Michard, A., El Kadiri, K., Negro, F., Frizon de Lamotte, D., Soto, J.I., and Saddiqi, O., 2008, The Rif belt, *in* Michard, A., and Saddiqi, O., eds., Continental Evolution: The Geology of Morocco Lecture Notes in Earth Sciences: Springer-Verlag Berlin, Heidelberg, p. 203–302, https://doi.org/10.1007/978-3-540-77076-3_5.

Durand-Delga, M., and Olivier, Ph., 1988, Evolution of the Alboran block margin from Early Mesozoic to Early Miocene time, *in* Jacobshagen, V.H., ed., The Atlas system of Morocco: Lecture Notes in Earth Sciences, v. 15, p. 463–480, https://doi.org/10.1007/BFb0011605.

Durand-Delga, M., Gardin, S., and Olivier, P., 1999, Datation des flyschs éocrétacés maurétaniens des Maghrébides: la formation du Jbel Tisirène (Rif, Maroc): Comptes Rendus de l'Académie des Sciences France, v. 328, no. 10, p. 701–709, https://doi.org/10.1016/S1251-8050(99)80180-3.

Durand-Delga M., and Maaté A., 2003, Illustration de la zone Tariquide au Jurassique: le rocher de Lechkrach, dans le Rif septentrional (Province de Tétouan, Maroc): Travaux de l'Institut Scientifique, Série Géologie et Géographie physique, v. 21, p. 127–134.

Zaghloul, M.N., Di Staso, A., Gigliuto, L.G., Maniscalco, R., and Puglisi, D., 2005, Stratigraphy and provenance of Lower and Middle Miocene strata within the External Tanger Unit (Intra-Rif sub-Domain, External Domain; Rif, Morocco): First evidence: Geologica Carpathica, v. 56, no. 6, p. 517–530.

Zaghloul, M.N., Di Staso, A., de Capoa, P., and Perrone, V., 2007, Occurrence of upper Burdigalian silexite beds within the Beni Ider Flysch Fm. in the Ksar-es-Seghir area (Maghrebian Flysch Basin, Northern Rif, Morocco): stratigraphic correlations and geodynamic implications: Bollettino della Società Geologica Italiana, v. 126, p. 223–239.

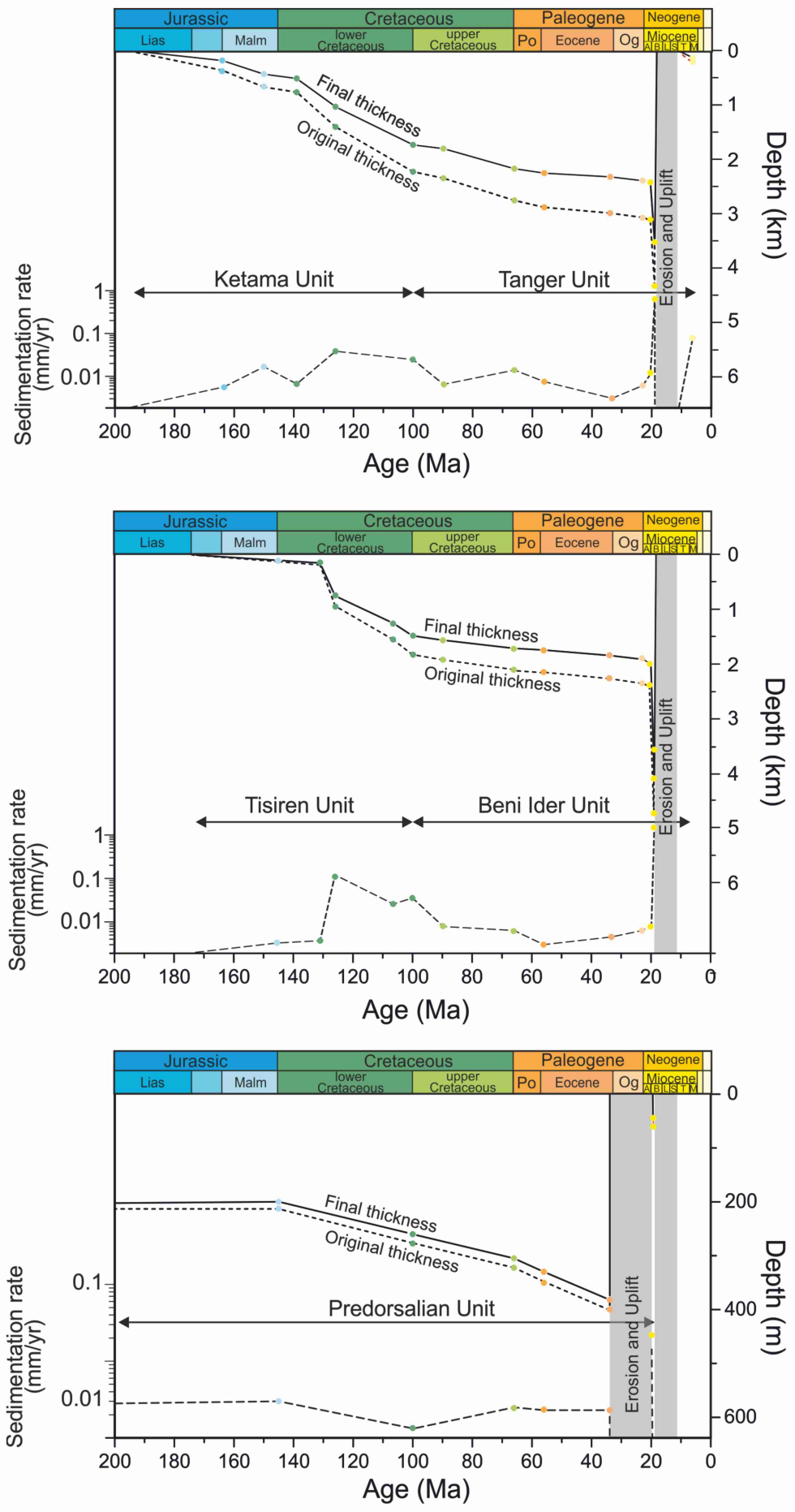
Jurassic
Cretaceous
Paleogene
Neogene
Lias
Malm
lower Cretaceous
upper Cretaceous
Po
Eocene
Og
Miocene
ABIJSTM
Final thickness
Original thickness
Erosion and Uplift
Ketama Unit
Tanger Unit
Tisiren Unit
Beni Ider Unit
Predorsalian Unit
Sedimentation rate (mm/yr)
Depth (km)
Depth (m)
Age (Ma)

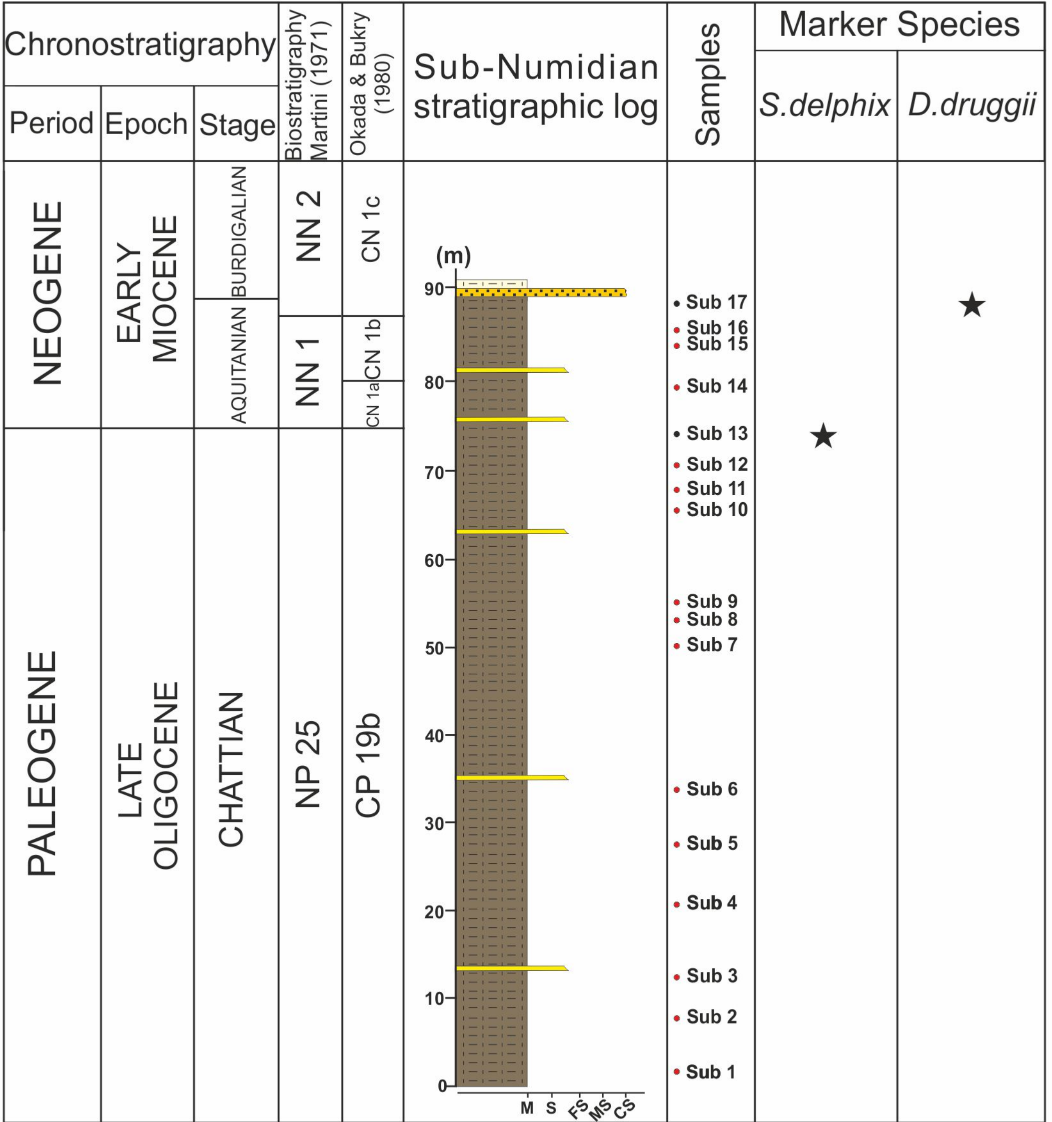

Chronostratigraphy
Period
Epoch
Stage
Biostratigraphy Martini (1971)
Okada & Bukry (1980)
Sub-Numidian stratigraphic log
Samples
Marker Species
S.delphix
D.druggii
NEOGENE
EARLY MIOCENE
BURDIGALIAN
AQUITANIAN
NN 2
NN 1
CN 1c
CN 1b
CN 1a
PALEOGENE
LATE OLIGOCENE
CHATTIAN
NP 25
CP 19b
(m)
90
80
70
60
50
40
30
20
10
0
M
S
FS
MS
CS
Sub 17
Sub 16
Sub 15
Sub 14
Sub 13
Sub 12
Sub 11
Sub 10
Sub 9
Sub 8
Sub 7
Sub 6
Sub 5
Sub 4
Sub 3
Sub 2
Sub 1

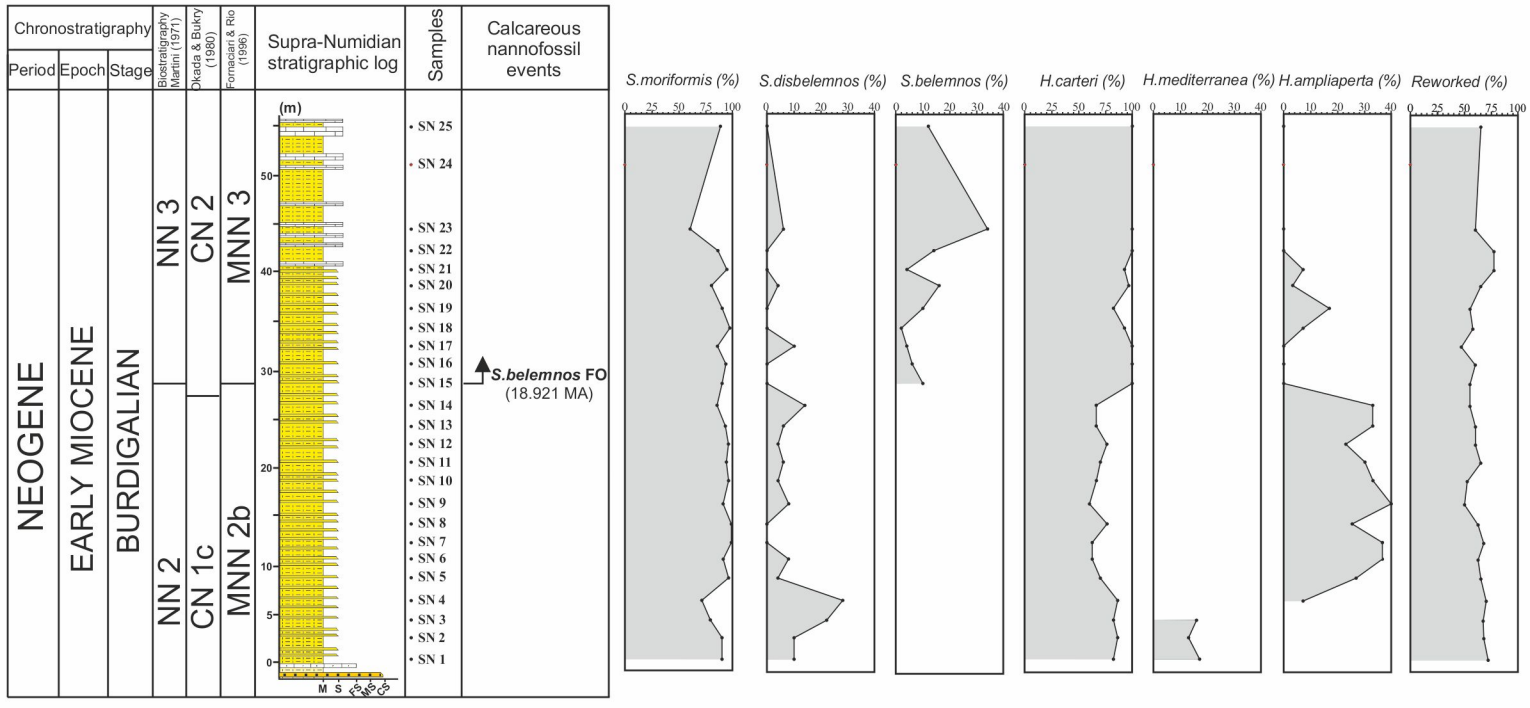
Chronostratigraphy
Period
Epoch
Stage
Biostratigraphy Martini (1971)
Okada & Bukry (1980)
Fornaciari & Rio (1996)
Supra-Numidian stratigraphic log
Samples
Calcareous nannofossil events
NEOGENE
EARLY MIOCENE
BURDIGALIAN
NN 2
CN 1c
MNN 2b
NN 3
CN 2
MNN 3
(m)
50
40
30
20
10
5
0
M
S
PS
MS
CS
SN 25
SN 24
SN 23
SN 22
SN 21
SN 20
SN 19
SN 18
SN 17
SN 16
SN 15
SN 14
SN 13
SN 12
SN 11
SN 10
SN 9
SN 8
SN 7
SN 6
SN 5
SN 4
SN 3
SN 2
SN 1
S.belemnos FO
(18.921 MA)
S.moriformis (%)
S.disbelemnos (%)
S.belemnos (%)
H.carteri (%)
H.mediterranea (%)
H.ampliaperta (%)
Reworked (%)
0 25 50 75 100
0 10 20 30 40

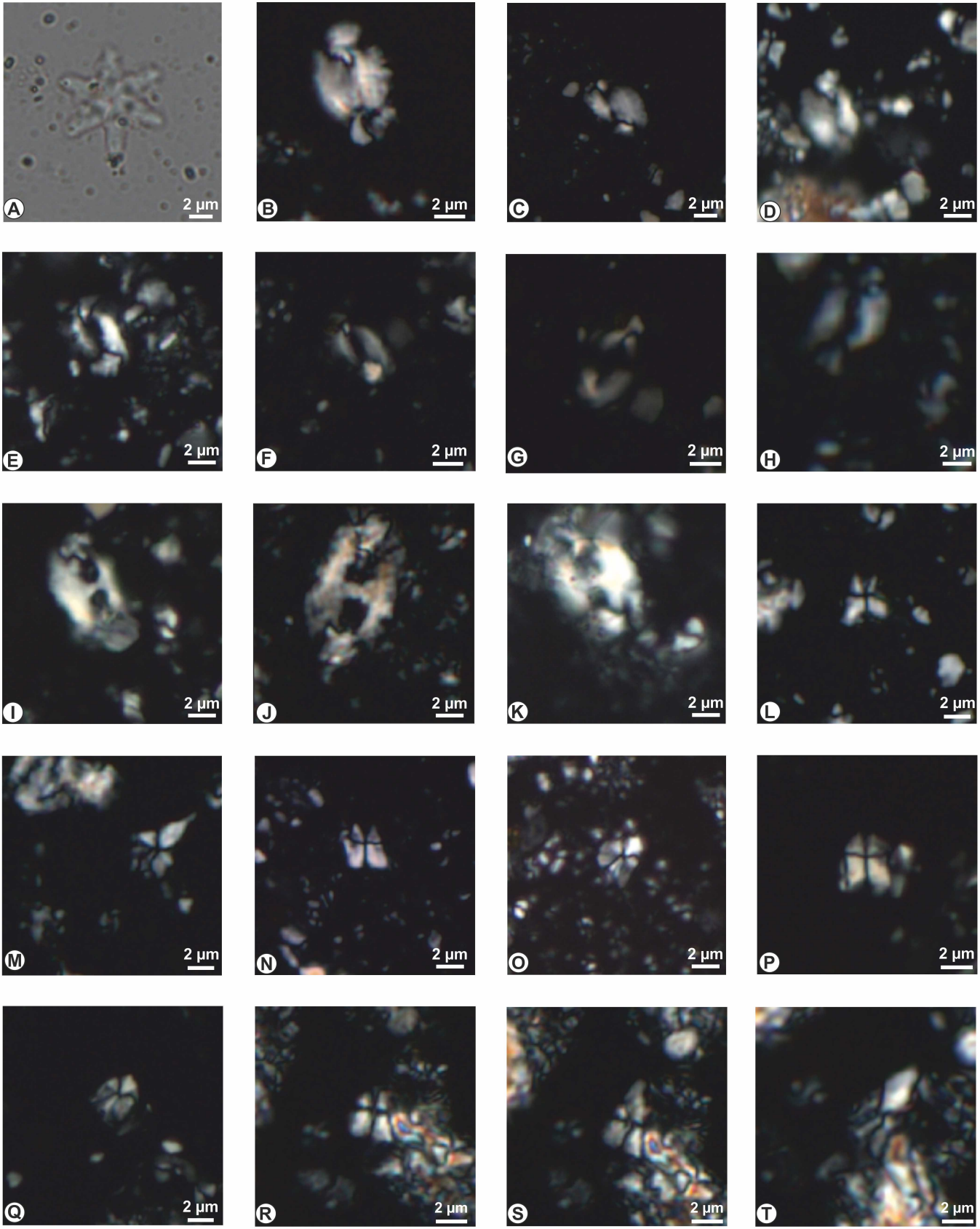
A
2 µm
B
2 µm
C
2 µm
D
2 µm
E
2 µm
F
2 µm
G
2 µm
H
2 µm
I
2 µm
J
2 µm
K
2 µm
L
2 µm
M
2 µm
N
2 µm
O
2 µm
P
2 µm
Q
2 µm
R
2 µm
S
2 µm
T
2 µm

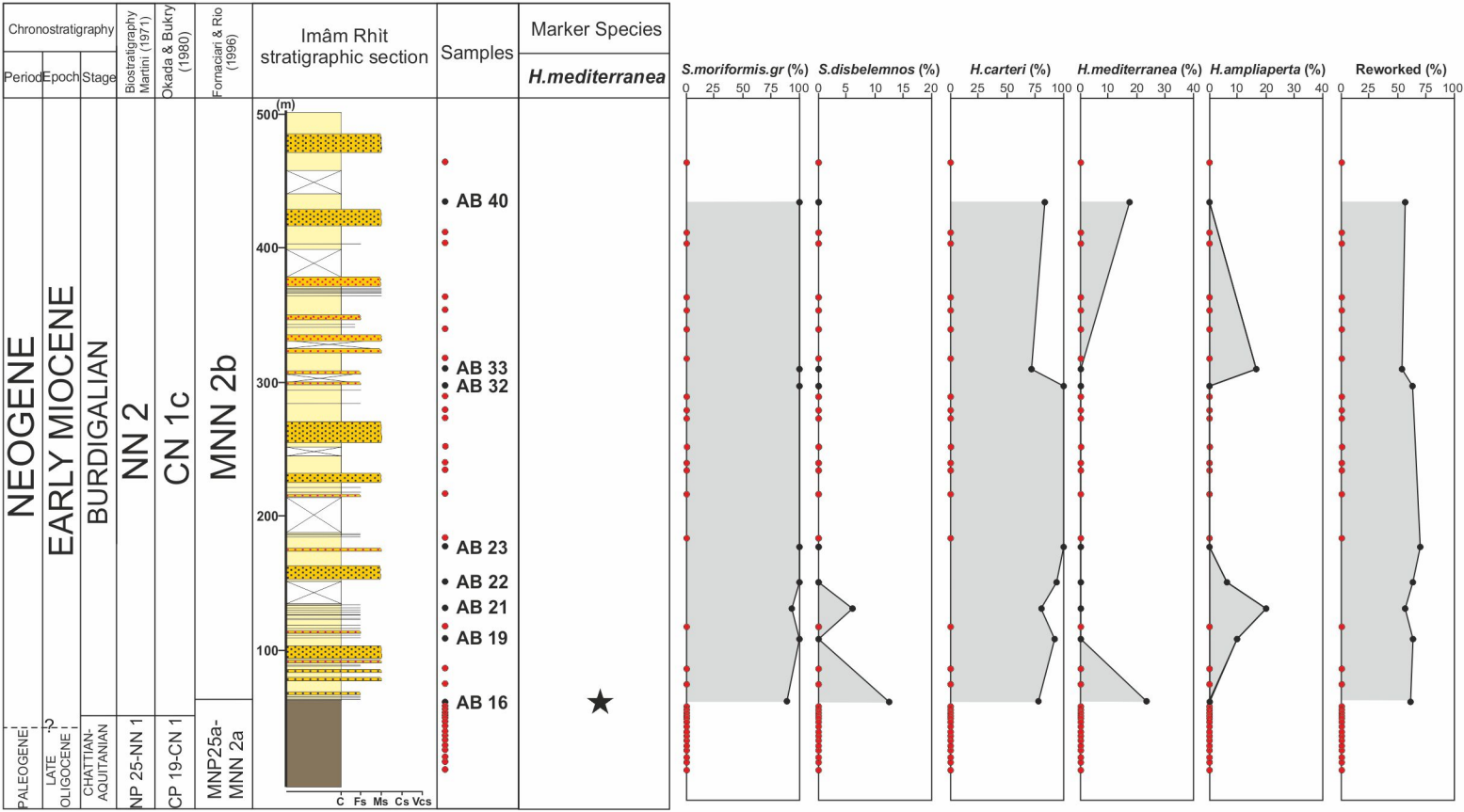
Chronostratigraphy
Period
Epoch
Stage
Biostratigraphy Martini (1971)
Okada & Bukry (1980)
Fornaciari & Rio (1996)
Imâm Rhît stratigraphic section
Samples
Marker Species
H.mediterranea
NEOGENE
PALEOGENE
?
LATE OLIGOCENE
EARLY MIOCENE
CHATTIAN-AQUITANIAN
BURDIGALIAN
NP 25-NN 1
CP 19-CN 1
NN 2
CN 1c
MNP25a-MNN 2a
MNN 2b
(m)
500
400
300
200
100
C
Fs
Ms
Cs
Vcs
AB 40
AB 33
AB 32
AB 23
AB 22
AB 21
AB 19
AB 16
S.moriformis.gr (%)
0 25 50 75 100
S.disbelemnos (%)
0 5 10 15 20
H.carteri (%)
0 25 50 75 100
H.mediterranea (%)
0 10 20 30 40
H.ampliaperta (%)
0 10 20 30 40
Reworked (%)
0 25 50 75 100

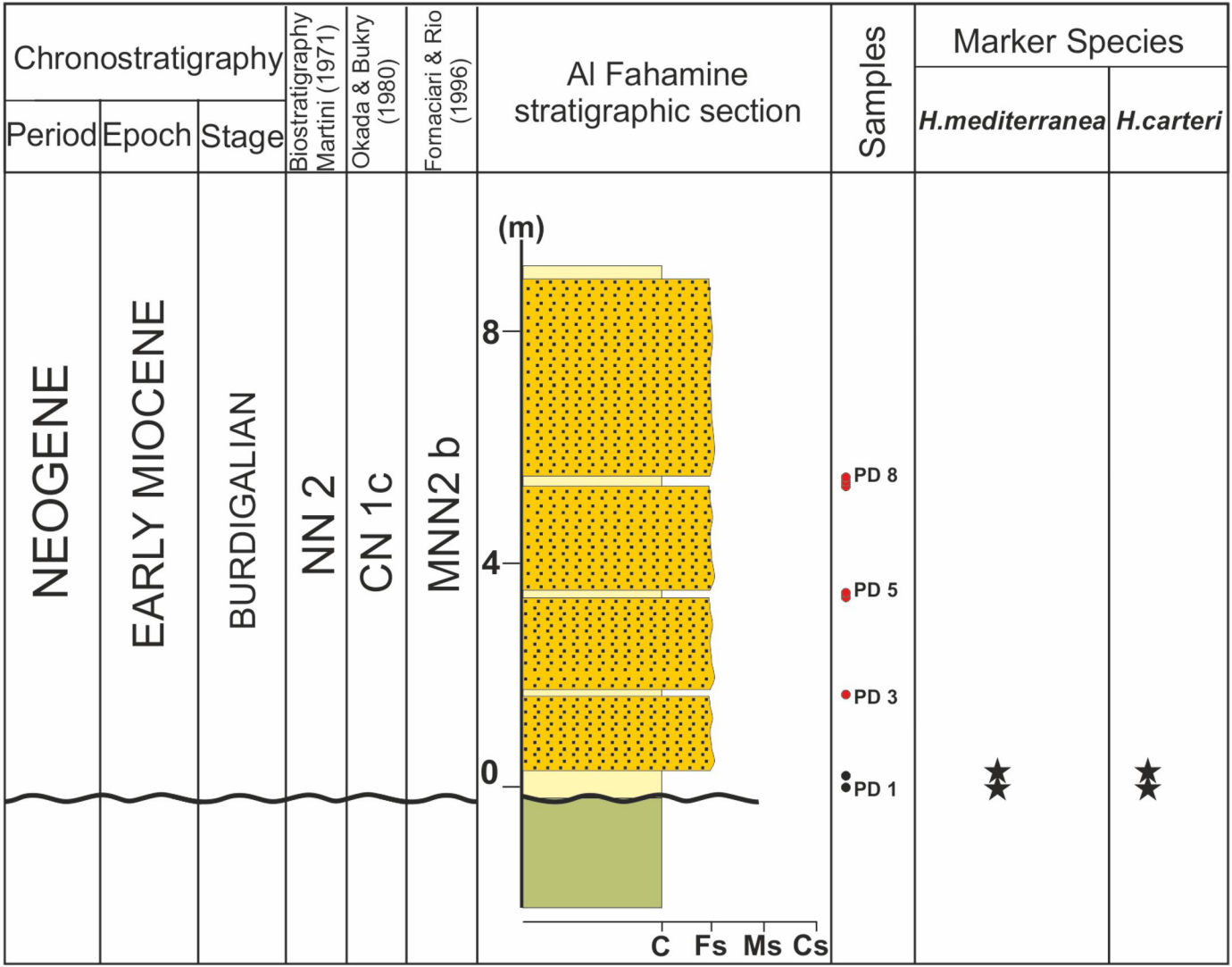
Chronostratigraphy
Period
Epoch
Stage
Biostratigraphy Martini (1971)
Okada & Bukry (1980)
Fornaciari & Rio (1996)
Al Fahamine stratigraphic section
Samples
Marker Species
H.mediterranea
H.carteri
NEOGENE
EARLY MIOCENE
BURDIGALIAN
NN 2
CN 1c
MNN2 b
(m)
8
4
0
PD 8
PD 5
PD 3
PD 1
C
Fs
Ms
Cs

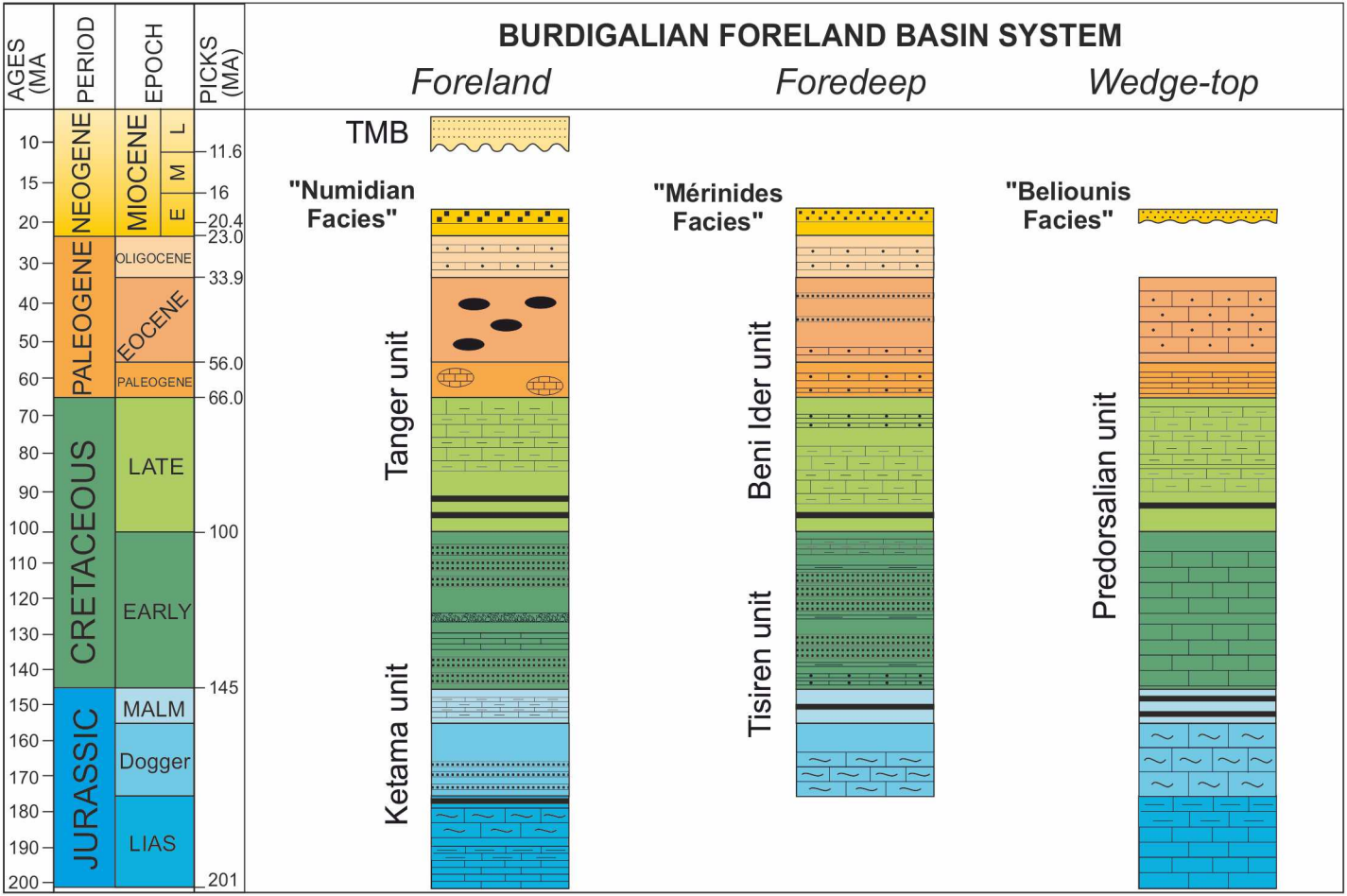
BURDIGALIAN FORELAND BASIN SYSTEM
Foreland
Foredeep
Wedge-top
AGES (MA
PERIOD
EPOCH
PICKS (MA)
NEOGENE
MIOCENE
L
M
E
11.6
16
20.4
23.0
PALEOGENE
OLIGOCENE
33.9
EOCENE
56.0
PALEOGENE
66.0
CRETACEOUS
LATE
100
EARLY
145
JURASSIC
MALM
Dogger
LIAS
201
10
15
20
30
40
50
60
70
80
90
100
110
120
130
140
150
160
170
180
190
200
TMB
"Numidian Facies"
Tanger unit
Ketama unit
"Mérinides Facies"
Beni Ider unit
Tisiren unit
"Beliounis Facies"
Predorsalian unit